A Description of the Pile Oscillators of DR1

Christensen, Peter Skjerk

Publication date:
1966

Document Version
Publisher's PDF, also known as Version of record

Risö Report No. 134

Risö Report No. 134

Danish Atomic Energy Commission

Research Establishment Risö

A Description of the Pile Oscillators at DR 1

by P. Skjerk Christensen

June, 1966

Sales distributors: Jul. Gjellerup, 87, Sölvgade, Copenhagen K, Denmark

Available on exchange from: Library, Danish Atomic Energy Commission, Risö, Roskilde, Denmark

June, 1966 Risö Report No. 134

A Description of the Pile Oscillators at DR1

by

P. Skjerk Christensen

The Danish Atomic Energy Commission
Research Establishment Risö
DR1

Abstract

A description is given of the pile oscillators at DR1 (a homogeneous reactor), together with the results of some measurements performed.

Two types of oscillators are in current use: a global and a local oscillator. The global oscillator is used in two positions; in the centre and at the edge of the core, in order to be able to separate the absorbing and the scattering properties of a given sample. The local oscillator is situated in the reflector of the reactor, and utilizes an annular boron-coated ionization chamber made at Risö.

The main parameters of the oscillators are:

A square wave movement of 70 cm stroke and 30 seconds period with a transfer time of 0.5 second.

A flux of some 10^8 n/cm^2/sec at a power of 15 w.

These conditions give the least noise, corresponding to the signal from 0.03 mm^2 absorber material (0.01 mg boron).

The ratio between absorption and moderation signals is 6.3 in the core centre and 14.5 in the local oscillator.

The epithermal index r is 0.1 at the core centre and 0.05 at the local oscillator.

Contents

1. Introduction

In this report the pile oscillators at the research reactor DR1 are described. There are two different pile oscillators in current use, a global oscillator in which the sample is oscillated in a tube penetrating through the core, and a local oscillator in which the sample is oscillated through an ionization chamber placed in the reflector of the reactor. In the global pile oscillator the sample affects the reactivity and thus the neutron density throughout the reactor, while in the local oscillator only the neutron density in the vicinity of the chamber is perturbed.

First a description of the reactor is given, whereafter follows a discussion of the two oscillators and finally reports are given of some measurements carried out with the oscillators.

2. The DR1 Reactor

The DR1 reactor is an aqueous homogeneous reactor. The core is spherical with a diameter of 32 cm, and contains 5 kg of uranium enriched 20% in U-235. Uranium in the form of UO_2SO_4 is dissolved in water, and the total core volume is some 14 litres.

The core is penetrated by a 1" diameter tube, which is welded to the core vessel. (See fig. 1A).

The graphite reflector surrounding the core is cylindrical. It has a diameter of 6 feet and is 5 feet high. Graphite stringers can be removed from the reflector and thereby 8 different experimental 4" x 4" holes can be obtained. Of these, four can be made into through-holes situated close to the core, while the remaining four only penetrate half way through the reflector.

The reactor is provided with a cooling system which keeps the temperature of the solution virtually constant (within a few hundreths of a degree centigrade), whereby the reactivity is almost constant. This is necessary because reactivity fluctuations due to temperature variations will influence the signal of the pile oscillator.

The reactor is provided with five control rods: two safety rods, two control rods operated by the reactor operator, and one control rod especially made for the pile oscillator and operated by the pile oscillator operator. The reactivity of this rod corresponds to a small fraction of one of the normal control rods. It is made of stainless steel and placed in one of the

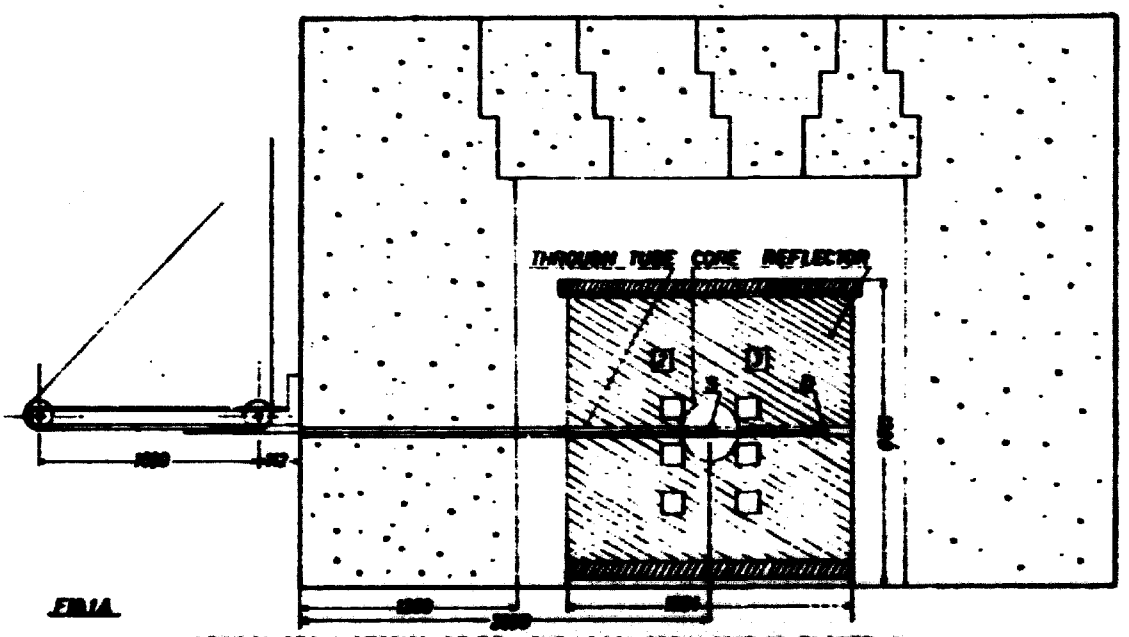

FIG 1A

VERTICAL CROSS SECTION OF DR 1. THE LOCAL OSCILLATOR IS PLACED IN EXPERIMENTAL HOLE NO 2, THE DETECTOR FOR THE GLOBAL OSCILLATOR IS PLACED IN HOLE NO 3. S IS THE SAMPLE CONTAINER AND B IS THE DUMMY OF THE GLOBAL OSCILLATOR.

FIG 1B

HORIZONTAL CROSS SECTION OF DR 1

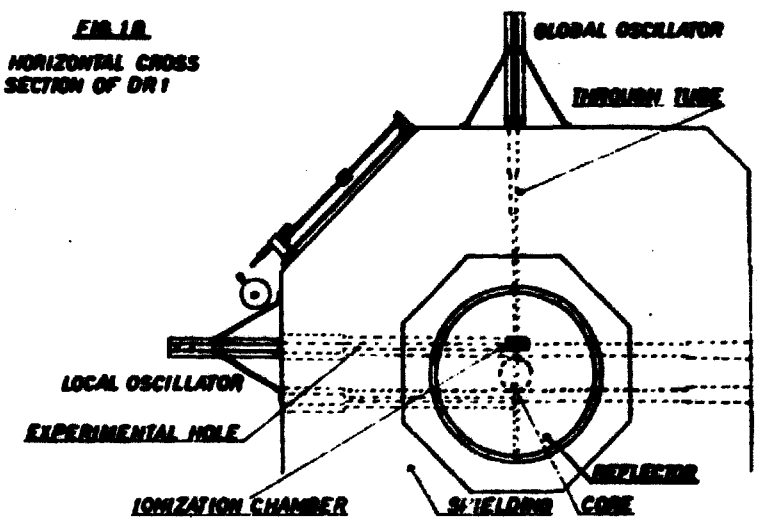

reflector holes.

The maximum power of the reactor is 2000 watts. This power level is determined by the permissible radiation level around the reactor. The flux in the centre of the reactor is 6×10^{10} n/cm^2/sec at 2000 watts.

However, when the reactor is used for pile oscillator measurements, the power is 15 watts only. This power level is regarded as the optimum when taking both noise and stability into consideration.

A more detailed description of the reactor is given in ref. 1.

3. Oscillators

In order to obtain well defined measurements, the sample movement should be carried out ideally in a square wave fashion, in which the movement takes virtually no time. In this way the signal is unaffected by the continuously shifting neutron spectrum through which the sample moves on its way from outside the reactor system to the measuring position.

In both oscillators the sample follows a nearly square wave motion with a period of 30 seconds. The movement takes half a second each way. Thus conditions are close to the ideal.

When using the global oscillator, the sample is moved between a position outside and a position inside the core, whereby the reactivity is modulated, which in turn results in a modulation of the reactor power. In the measurements, only the amplitude and the phase of the first harmonic, as determined by a Fourier analysis, are of interest. Therefore the output from an ionization chamber is multiplied by a sine and a cosine and integrated over an appropriate number of periods.

In the local oscillator the sample is moved between a position outside the reactor and a position in the reflector where the flux perturbation, produced in the vicinity of the sample, is determined by an ionization chamber. The global effect is negligible and is of no interest. The output from the ionization chamber is processed similarly to that of the global oscillator.

3.1. Mechanical Arrangements

The arrangement is shown on fig. 1A and 1B, where a cross section of the reactor and the positions of the ionization chambers are given. The global oscillator is installed in the through-tube. In order to have a smooth surface for the movement of the sample container, an aluminium tube (oscillator tube) is inserted into the through-tube, (see fig. 2). In the part of

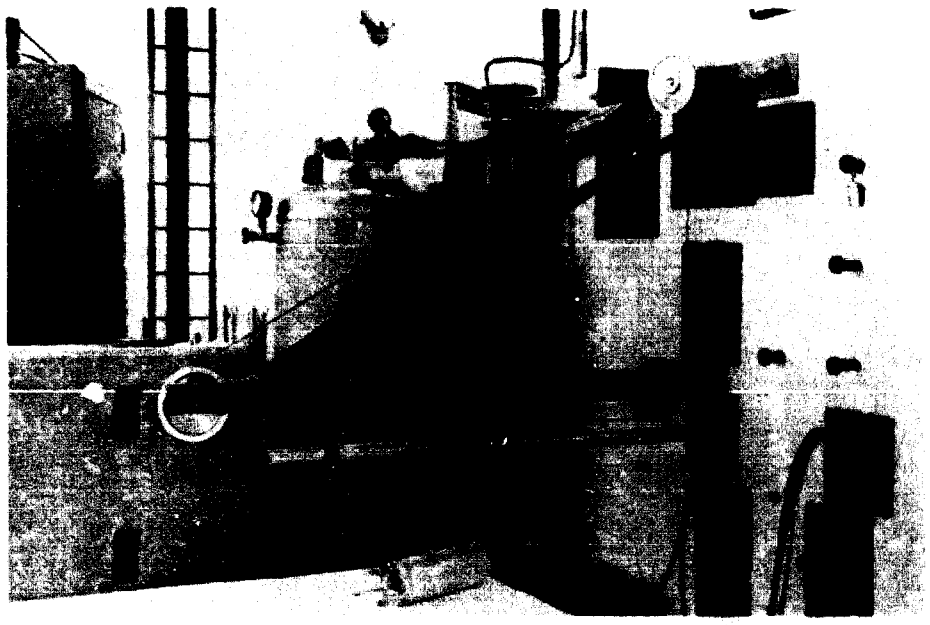

Fig. 1C. The local oscillator. The driving mechanism (fig. 6A) in the background. The oscillator rod is in the outer position. An annular ionization chamber is placed on the table.

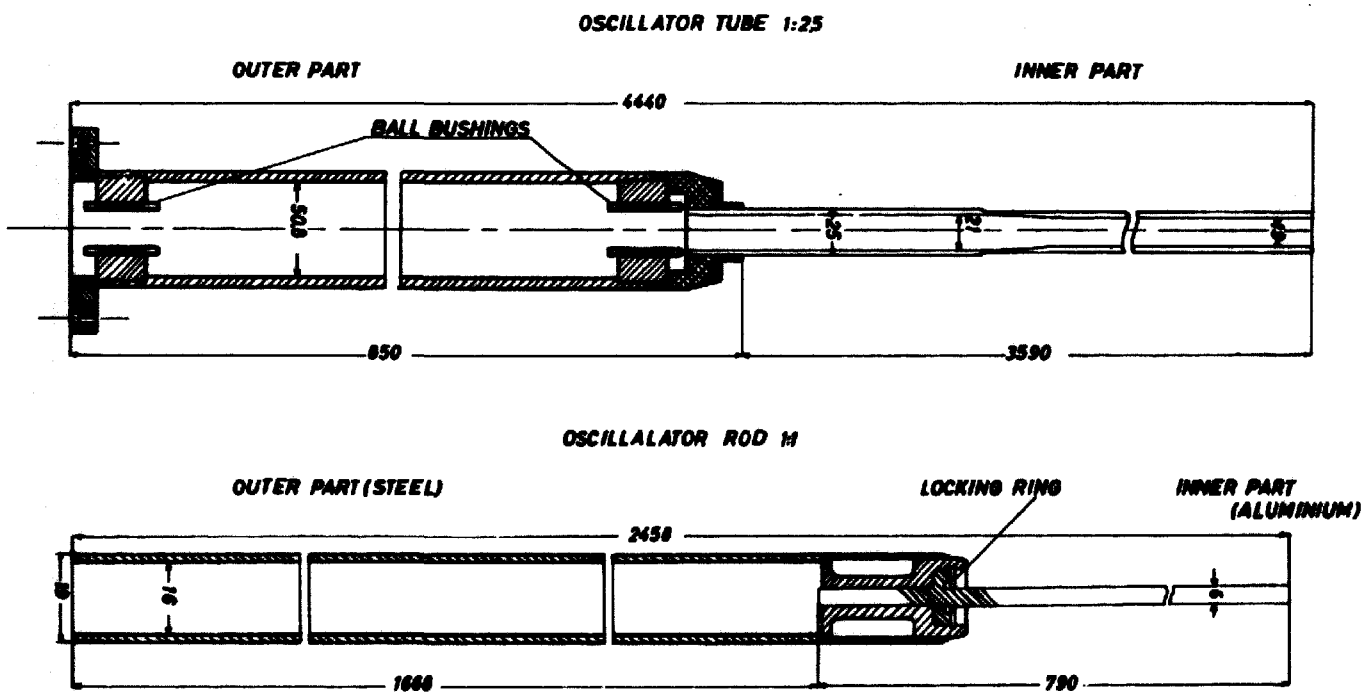

FIG 2

MAIN PARTS OF GLOBAL OSCILLATOR

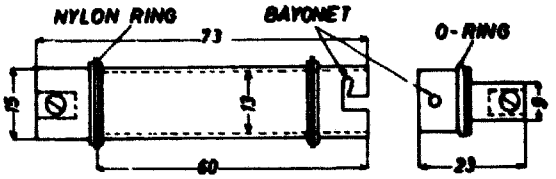

CONTAINER OF ALUMINIUM FOR SOLID SAMPLES

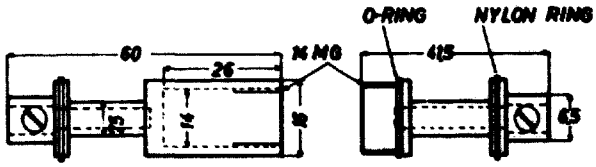

CONTAINER OF ALUMINIUM FOR LIQUIDS AND SOLIDS

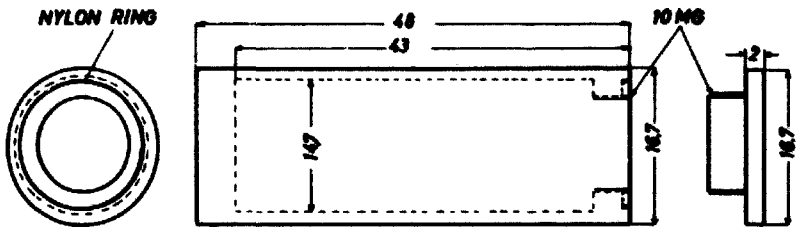

CONTAINER OF ALUMINIUM FOR LIQUIDS TO BE PLACED IN THE NYLON CARRIER SHOWN BELOW

NYLON CARRIER FOR SOLID SAMPLES AND FOR THE CONTAINER SHOWN ABOVE

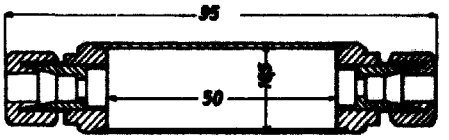

FIG 3

SAMPLE CONTAINERS FOR THE GLOBAL OSCILLATOR

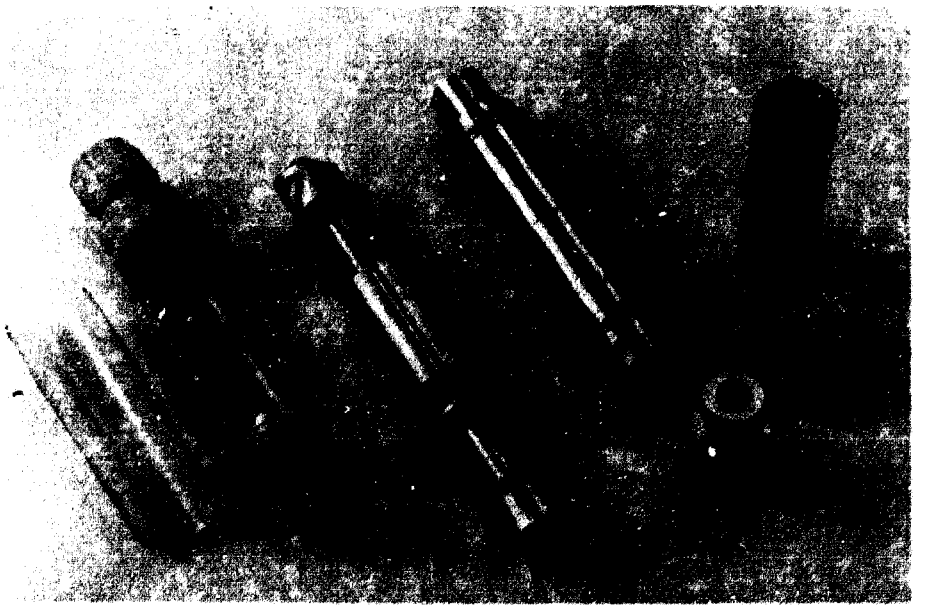

Fig. 3A. Sample containers for the global oscillator. From left: nylon container for solids; 2 cm Al-container for liquids; Al-container for solids; polyethylene container for liquids.

the tube situated in the shield, two ball-bushings are placed in which the outer part of the oscillator rod runs. The oscillator rod, moving in the oscillator tube, is composed of an outer 19 mm steel tube connected to an inner 1/4" aluminium tube by a locking ring (see fig. 2). The sample container is fixed to the end of this tube.

As the container itself has a certain effect on the signal, a dummy container is attached to the sample container with a 1/4" aluminium rod of a length equal to the length of the oscillator stroke, normally 70 cm (see fig. 1A). The dummy is adjusted so as to cancel the effect of the container.

Depending upon the properties of the sample (solid or liquid) different types of sample containers are used (see figs. 3 and 3A).

The sample container has a smooth outer surface in order to reduce the friction between itself and the oscillator tube. Normally nylon is used; the sample container being either entirely made of nylon or provided with rings of nylon if made of other materials. The dummy is identical to the sample container. The maximum length of the sample is determined by the influence function of the reactor and depends upon the position in the reactor to which the sample is moved. When moved to the centre of the reactor, the sample is usually 5 cm long, whereas it is only 2 cm when measurements are performed at the edge of the core.

The local oscillator is located as shown in figs. 1A and 1B, and fig. 1C gives a view of the oscillator. A rig containing the oscillator is placed in the reflector with the ionization chamber in the symmetry plane of the reactor. However, the set-up is not entirely symmetrical as there is solid graphite at the one end of the chamber while the oscillator tube penetrates the graphite from the other end, thereby permitting some neutron streaming. This may give rise to a signal from scattering materials at the ends of the chamber. The annular ionization chamber is part of the rig which is shown on fig. 4. The remaining parts of the local oscillator are similar to those of the global oscillator, i. e. the aluminium oscillator tube in which the sample container slides, the oscillator rod attached to the driving wire and running on nylon bearings (no lubrication necessary), and the extension tube forming the connection between the container and the oscillator rod. It is not possible to use a dummy in the local oscillator, because the hole used is not a through-hole. The position was chosen because it is distant from the core, whereby the interaction between the sample and the core is small, and because the neutron spectrum is soft compared to that in the core centre. The sample containers for the local oscillator are similar to those used in the global oscillator. They are shown on figs. 5 and 5A.

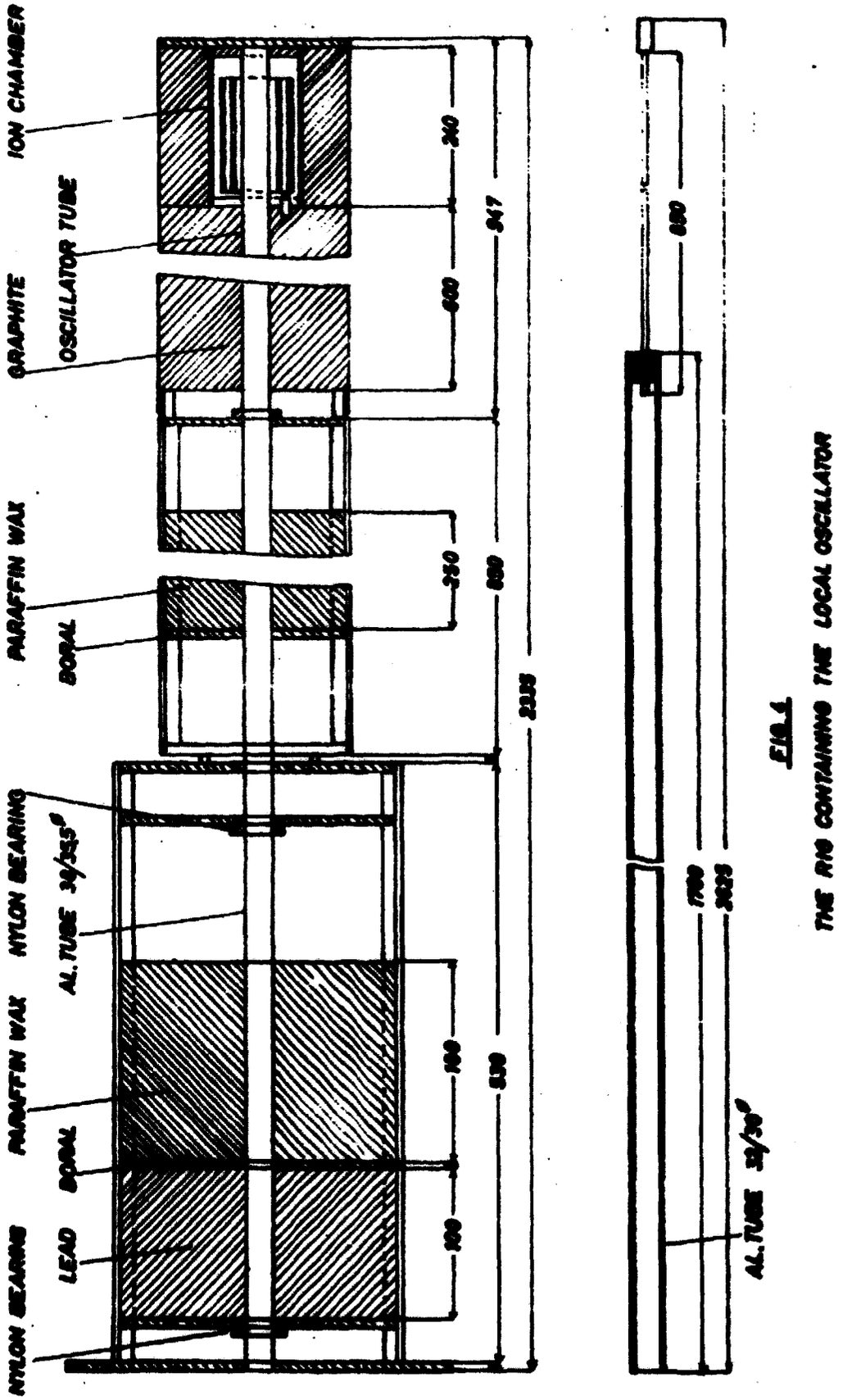

FIG. 1

THE RIG CONTAINING THE LOCAL OSCILLATOR

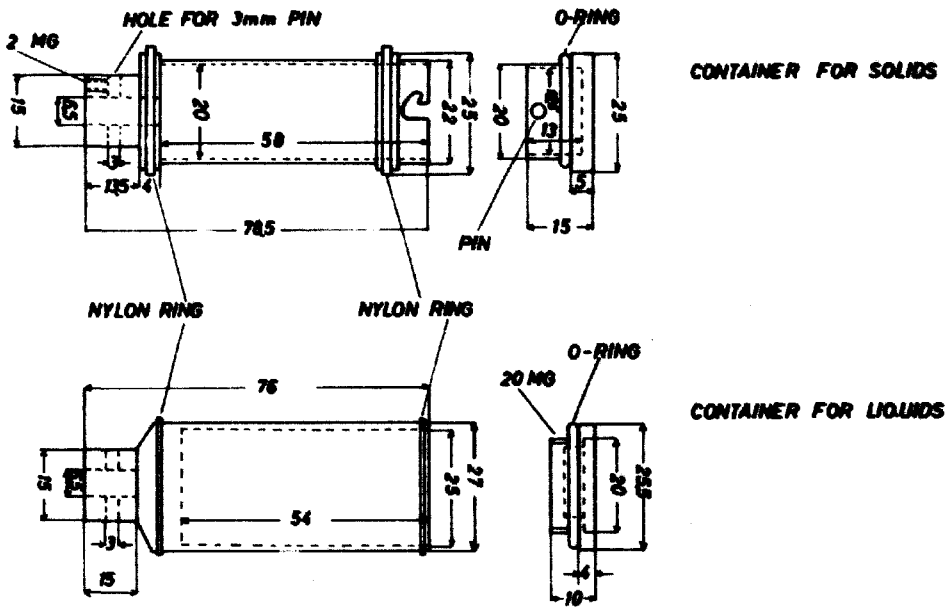

FIG 5

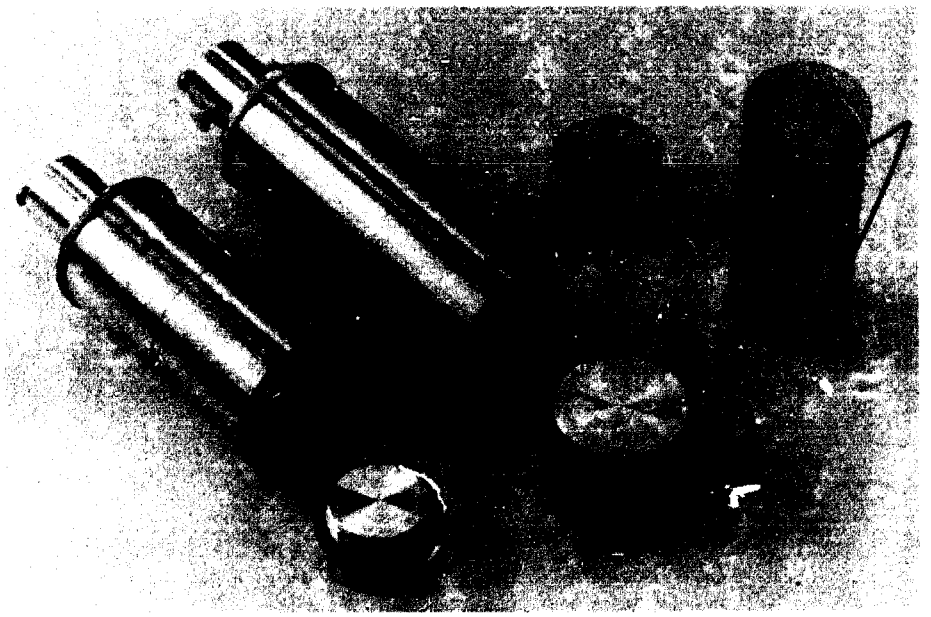

Fig. 5A. Sample containers for the local oscillator. From left: Al-container for liquids; Al-container for solids; polyethylene container for liquids with locking device.

The same driving mechanism is used for both oscillators and is simply shifted from one to the other by changing a wire. It is composed of the following parts:

a) A timing motor and cam-drive activating relays through microswitches. This determines the movement of the rod and drives the analyzing equipment.

b) A compressed-air cylinder moving the oscillator rod to which it is attached by a wire.

The timing motor is an asynchroneous motor running with nearly constant speed because of the constant friction in the gears. The output speed may be set to certain values by changing some gear wheels. The normal speed is 2 r.p.m. There are some cam wheels fixed to the slow running shaft and microswitches are activated by these wheels; in addition, it drives the sine and cosine potentiometers through a crank shaft. Magnetic valves activated by some of the microswitches govern the compressed air for the cylinder (fig. 6). The cylinder drives the oscillator rods through wires and some microswitches attached to the moving part of the drive mechanism provide the cylinder with breaking air near the end of the stroke, so that the rods will stop gently at the end of each stroke. Fig. 6A pictures the driving mechanism.

The movement of the sample has been investigated by filming the rod during the stroke. A camera was used which ran at a speed of 64 frames per sec. It viewed a scaler, fed with a 100 cps signal, and simultaneously the outer part of the oscillator rod. The result is given on fig. 7, where it is seen that the speed of the rod during oscillations is reproduced rather well. The results also shown that it takes a relatively long time to bring the sample to rest at the end positions. But as the stopping time seems to be the same for all strokes, this is insignificant.

Some other experiments have shown that the measuring position was reproduced quite well, the maximum deviation being 1/4 mm.

3.2. Electrical Arrangement

The ionization chambers are placed as shown on fig. 1A.

The analyzing equipment, common to the two oscillators, consists of a DC-amplifier, sine-cosine-multipliers, and integrators (fig. 8).

The DC-amplifier is of normal design and is equipped with balanced circuits throughout in order to minimize the drift. The amplification may

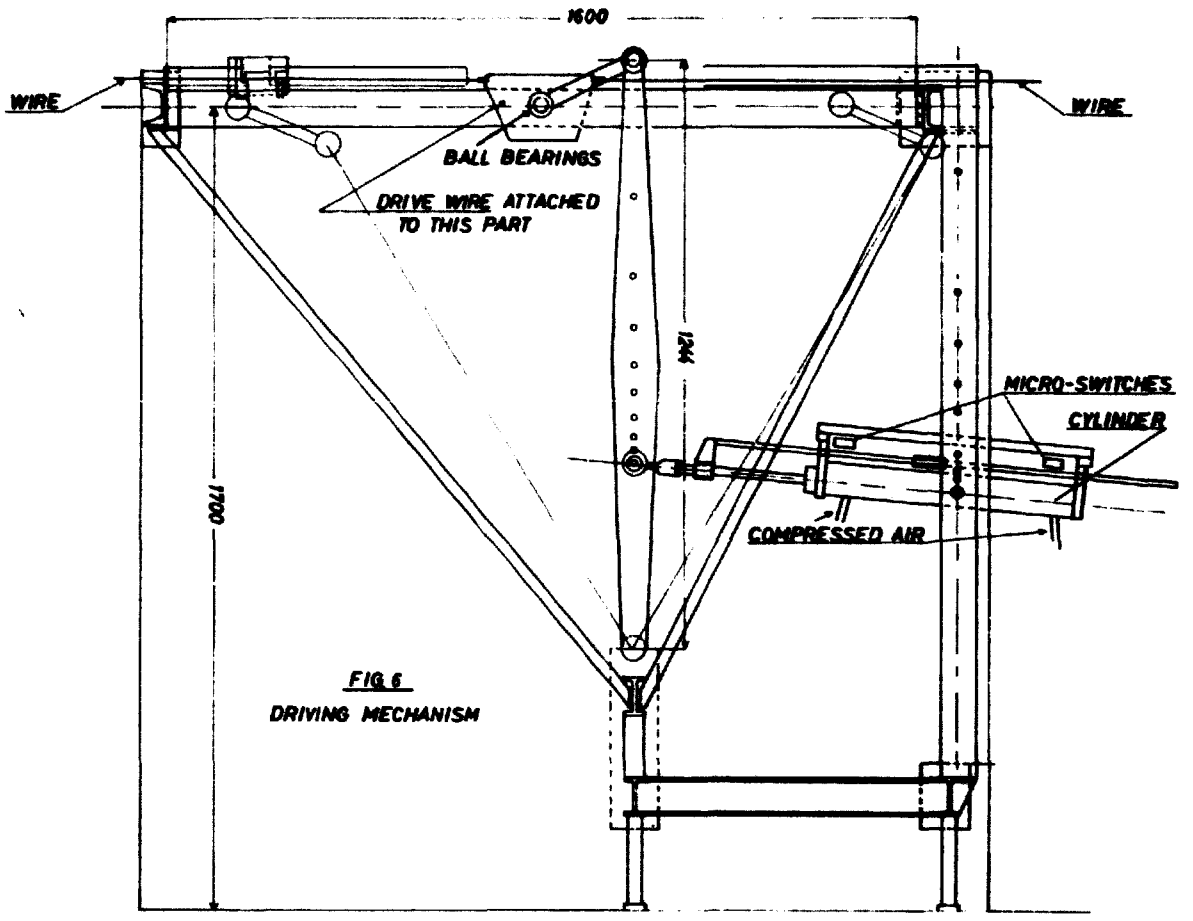

FIG 6
DRIVING MECHANISM

Fig. 6A. The driving mechanism. A storage container for compressed air is seen to the right. Magnetic valves are seen below the cylinder.

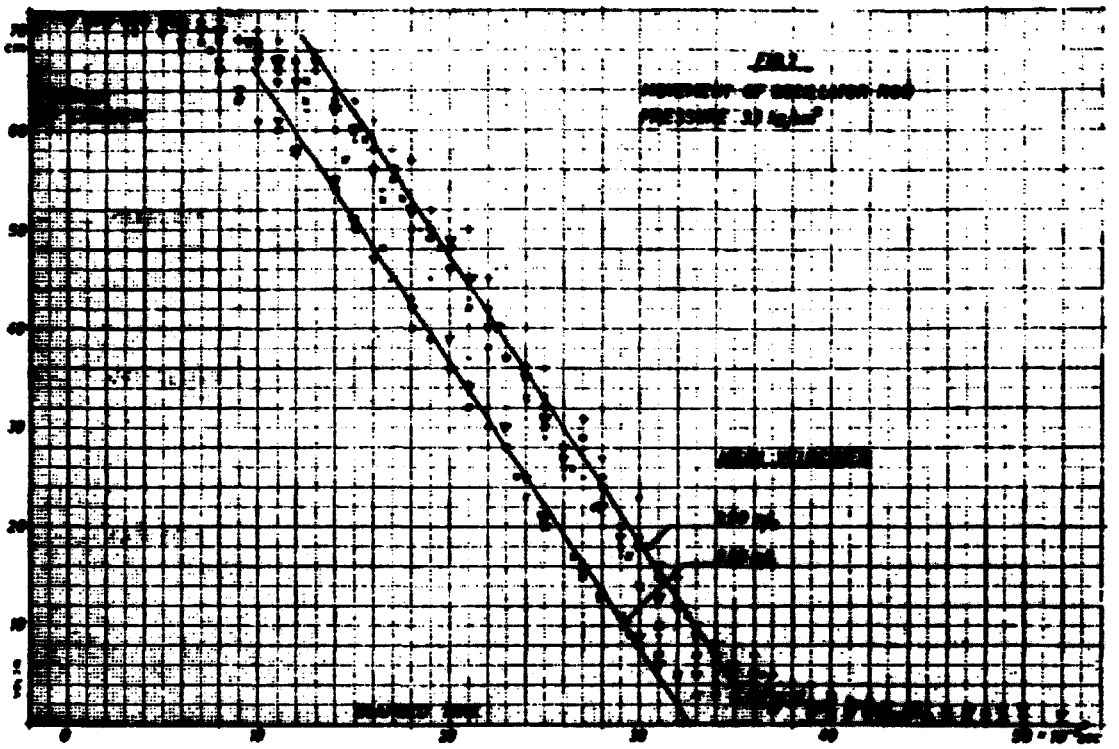

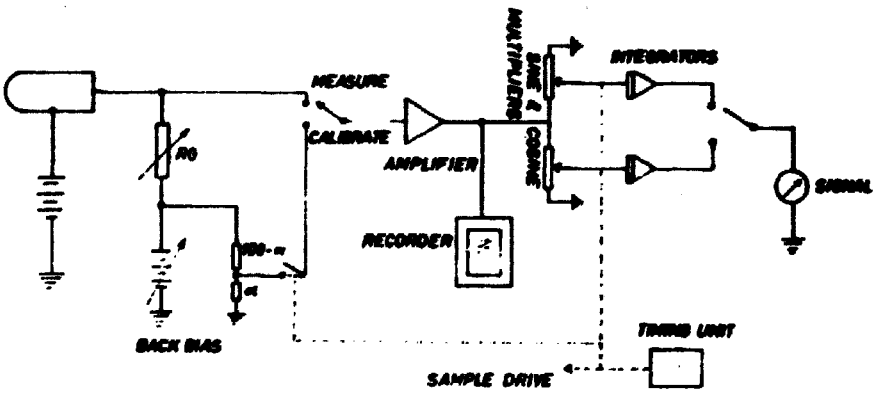

FIG 6

SCHEMATIC DIAGRAM OF THE PILE OSCILLATOR ANALYSING EQUIPMENT

be varied in the range of 48 - 63 db. The load resistance is variable in the range 0.01 - 50 M-ohm, and a back-bias is provided in order to suppress the DC-component of the ion chamber current. Part of the back-bias may be fed through the amplifier by means of a switch, and it is chopped with a relay activated by the timing unit in order to give a calibration output which is used to correct the signal for changes in the mean level of the reactor power and changes in the amplification.

A recorder is connected to the output of the amplifier. The operator uses the recorder when stabilizing the reactor with the special control rod. The output from the amplifier is also fed to two multipliers (sine and cosine) consisting of potentiometers, driven by a timing motor through a crank-shaft.

The integrators are made of conventional operation amplifiers provided with suitable RC-networks. The integration is timed by means of the timing unit.

The output is read on a precision voltmeter with a large scale, some twenty centimeters long. It has not been considered necessary to use any device, such as a digital voltmeter, to read the output because the scale of the meter used can be read with an accuracy which corresponds to the noise of the signal.

3.3. Processing of the Measurements

The signals used are the voltages from the sine and cosine integrators. As the amplitude of the modulation of the reactor power is proportional to the power, the output from the integrators will also be proportional to the reactor power. Thus, as the average level of the input of the amplifier is cancelled by means of the back-bias voltage, a fraction α of the back-bias may be sent through the amplifier to obtain an output proportional to the average power level and which can be used to calibrate the equipment. The results from the sine and cosine channels to be used, S_{cos} and S_{sin}, are calculated from the following expression

$$S = \frac{V_m}{n_m} \cdot \frac{n_c}{V_c} \cdot \alpha \qquad (1)$$

where V_m is the voltage from the sample run integrated over n_m periods, V_c is the voltage from the calibration run integrated over n_c periods, and α is the fraction of back-bias used.

The quantity to be used to calculate the nuclear properties of the

sample is the amplitude of the first harmonic of the modulation, S,

$$S^2 = S^2_{cos} + S^2_{sin} \tag{1A}$$

There are some simple means of cancelling certain sources of error in the apparatus. One is the use of a calibration voltage, V_c, which cancels day-to-day changes of the amplification. Another is the timing of the beginning of the integration relative to the phase of the sine-cosine-multiplication which cancels the influence of a change of the mean neutron level, if this change is linear with time. It is possible to cancel higher order drift by special arrangements, (eq. ref. 9), but this was not felt worthwhile since the reactor normally runs quite steadily.

The efficiency of these circuits has been examined by measurements of pure noise and of some standard samples while the power varied linearly with time. The efficiency was found to be satisfactory since the variance of the signal measured when the power is decreasing or increasing is similar to that measured when the power is constant.

The signal consists of the modulation generated by oscillating a sample and the inherent noise from the reactor itself. Thus an "exact" signal S, free from noise cannot be obtained. It is assumed that the signal from a single measurement is normally distributed around the mean value, and thus a variance can be attached to the signal in the following way:

$$\sigma^2 = \frac{1}{n(n-1)} \sum_{i=0}^{n} (S_i - \bar{S}) \tag{2}$$

where

$$\bar{S} = \frac{1}{n} \sum_{i=0}^{n} S_i \tag{3}$$

Normally a sample is measured 4 consecutive times (n = 4).

For a given material the signal per gram, s_1, is of interest. To obtain s_1, samples of different weights must be measured, and the amount of sample material must be chosen so that self-shielding is kept low since self-shielding limits the amount of sample material and not the non-linearity of the reactor system (see section 3.4).

The experimental results are fitted together by a least squares fit to give s_1 and the standard variance of s_1. The following expressions have been used to fit to the mean values of the measurements: ($\bar{S} = \bar{S}(v)$):

$$\bar{S}(v) = s_o + s_1 v + s_2 v^2 \quad \text{(quadratic fit)} \tag{4}$$

$$\bar{S}(v) = s_o + s_1 v \quad \text{(linear fit)} \tag{4a}$$

where v is the weight of the sample. This procedure is carried out by use of a computer programme giving, in addition, the variance on each of the factors s.

The choice between the two fits is generally easy, either because samples without self-shielding have been used or because the self-shielding is heavy. However, there are cases where the two fits seem to be of equal confidence and here the variance of the quadratic member of (4) may determine the decision.

The signal, s_1, is a superposition of several properties of the material, namely the absorption, the scattering, and the moderation. However, only a single result is obtained from a certain material when measured in a given position. It may be written in the following way:

$$s_1 = \alpha \frac{\Sigma_a}{\rho} + \beta \frac{\Sigma_s}{\rho} + \gamma \frac{\xi \Sigma_s}{\rho} \tag{5}$$

where

$\frac{\Sigma_a}{\rho}$ is the absorption per gram of the sample,

$\frac{\Sigma_s}{\rho}$ is the scattering per gram,

$\frac{\xi \Sigma_s}{\rho}$ is the slowing down per gram,

and

s_1 is the signal from the oscillator per gram.

α, β, and γ are three parameters which must be determined, experimentally or theoretically. They depend primarily upon the position of the sample and of the duration of the movement.

In principle, only three materials with different known properties need to be measured in order to compute α, β, and γ. In practice, however, it is necessary to measure a number of different materials, whereafter an appropriate fitting procedure must be performed to give α, β, and γ, and the variance on each of these quantities. Such a procedure has been worked

out for the GIER computer of the Danish AEC using a standard least squares fit (e.g. ref. 10).

On the other hand, if the properties of a given sample must be determined, it is necessary to determine s_1 in three positions with different properties, from which it is possible to work out Σ_a/ξ , Σ_s/ξ , and $\xi\Sigma_s/\xi$, at least in principle.

3.4. Linearity

Usually, one anticipates linearity between the cross section of the sample, the modulation of the power, and the signal. However, two factors affect the linearity, namely self-shielding in the sample and non-linearity of the reactor. The former is dealt with in section 3.3 and the latter is examined here.

The kinetic equations of a point model reactor are usually written in the form:

$$\frac{dn}{dt} = \left[k_{eff}(1 - \varepsilon\beta) - 1\right] \frac{n}{l} + \Sigma_i \lambda_i C_i$$

$$\frac{dC_i}{dt} = \varepsilon_i \beta_i k_{eff} \frac{n}{l} - \lambda_i C_i$$

where

n is the neutron density

β_i is the fraction of delayed neutrons born in the i'th group, $\beta = \sum_i \beta_i$

λ_i is the decay constant of the emitters in the i'th group

ε_i is the weight of the neutrons in the i'th group

l is the prompt neutron life time

k_{eff} is the effective multiplication constant.

If the expressions for the relative variation of k_{eff}, q, and for the relative neutron density, p, are inserted into the equations, the following expressions are obtained after elimination of second order members (ref. 6):

$$\frac{dp}{dt} = \frac{1}{l} q - \frac{\varepsilon\beta}{l} p + \frac{1}{l} qp + \sum_i \lambda_i C_i$$

$$\frac{dC_i}{dt} = -\lambda_i C_i + \frac{\varepsilon_i \beta_i}{l} p$$

It is seen that the equation contains the non-linear member $\frac{1}{l} qp$.

By insertion of a sine wave $q = q_o + q_1 \sin \omega t$, and the nuclear constant for DR 1 into these equations the following expressions are found:

$$\frac{r_1}{r_{10}} \approx 1 - C_3 q_1^2 = 1 - 4.7 \times 10^3 \; q_1^2$$

$$r_2 \approx \frac{q_1^2}{2C_1C_2} = \frac{1}{1.4 \times 10^4} q_1^2$$

where

r_{10} is the linear response of the first harmonic,

r_1 is the response of the fir t harmonic including the most important non-linear member,

r_2 is the response of the second harmonic,

C_1, C_2, C_3 are constants depending on the delayed neutrons and the frequency.

The expressions show that the non-linearity becomes significant (1% decrease of the output) when $q_1 \sim 2 \times 10^{-3}$.

The same equations were solved on an analogue computer. The reactivity input variation was a square wave. It was found that when $q \sim 0.5 \times 10^{-3}$ the non-linearity amounted to 1%. The cross section corresponding to this reactivity amounts to half a cm^2. In practice, this limit will never be reached because of self-shielding in the sample.

Thus it can be concluded that the non-linearity of the reactor will normally be more significant than the self-shielding.

4. Determination of the Best Conditions for the Measurements

The quality of a measurement is determined by the variance of the signal and, as this is a measure of the noise in the system, conditions must be chosen for the experiments that give the least noise. As it is desirable to carry out the greatest number of measurements per day, the conditions must be selected so as to give the least noise in a given time.

4.1. Noise Measurement

In DR 1 the noise stems from two main sources, namely the random time-distribution of the fissions, and from the voids formed by the gas production in the core solution. The former gives the main contribution at low power, while the latter dominates at higher reactor powers. Thus a certain value of the power can be expected at which the noise is minimum.

The noise has a certain spectral distribution (which obviously depends upon the reactor power) and thus the noise signal as measured with the oscillator depends upon the period of the oscillations.

The noise has been measured with the pile oscillator equipment, but without oscillating anything in the reactor. The period and the power have been varied between certain limits. The results are shown on fig. 9 which clearly indicates that for a given oscillator period there is a power level which gives minimum noise. In addition, this minimum is seen to be a slowly varying function of the period.

This leads to the conclusion that a period of 30 seconds and a power of some 20 watts would be the optimum. However, it should be mentioned that this examination does not take into account the time elapsing from the start of the cooling system until the reactor is stable at the power used in the experiments. This time depends upon the power and is nearly one hour at 20 watts.

In addition to these measurements, detection of possible noise coming from the cooling system was attempted, but without giving any positive results. The cooling coil is situated inside the core tank in a region with a rather high statistical weight. Bubbles from the cooling pump may arrive in the core and collapse there, thereby giving rise to a reactivity change. However, changes in the coolant flow did not have any effect on noise measurements, and thus it was concluded that this noise is negligible.

The equivalent absorption cross section of the noise has been found to be 0.02 - 0.03 mm^2 in both of the oscillators. This figure gives the lower limit of the cross section which can be measured.

A theoretical estimate of the noise was made following the method of Littler[5] and gave a value of 0.05 mm^2. The agreement with the experimental values may, however, be fortuitous.

4.2. A Note on the Transfer Function

It has been calculated[7] that the transfer function depends upon the reactor power in such a way that when above a certain power the transfer

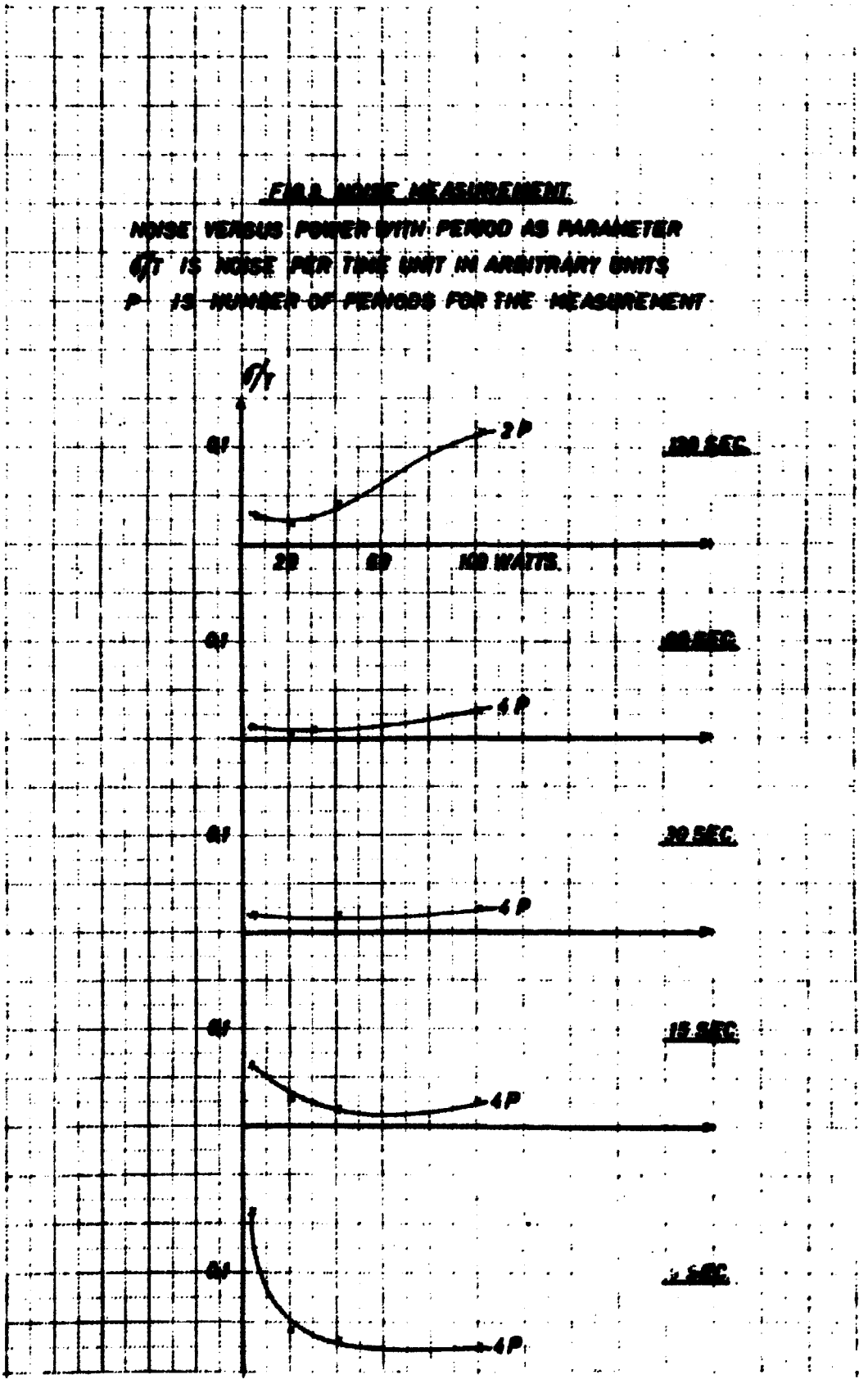
F/G 3. NOISE MEASUREMENT.
NOISE VERSUS POWER WITH PERIOD AS PARAMETER
δf/f IS NOISE PER TIME UNIT IN ARBITRARY UNITS
P IS NUMBER OF PERIODS FOR THE MEASUREMENT
δf/f
2 P
100 SEC.
20
60
100 WATTS.
4 P
60 SEC.
4 P
30 SEC.
4 P
15 SEC.
4 P
4 P

function will have a maximum, and that this maximum will move against higher frequencies when the power level is increased.

In addition, a series of calculations and experiments on the behaviour of DR 1 when a disturbance is introduced into the reactor system have been carried out. The behaviour can be described by a damped oscillation characterized by a frequency and a damping constant. It was shown that the frequency increased with increasing reactor power in accordance with the calculations mentioned above.

The frequency of these oscillations corresponds to a period of some 600 seconds at high power (2 kW), that is an order of magnitude larger than the normal pile oscillator period. This may explain the behaviour of the noise curves: When the power rises from zero, the relative noise will at first decrease, because an increasing number of fissions will give less noise which is proportional to $1/\sqrt{P}$, while it will increase later on because the maximum of the transfer function moves towards the analyzing frequency and so does the peak in the noise spectrum.

5. Global Oscillator

Two interesting positions have been found in the through-tube of the reactor where a calibration has been performed. In order to be of use, a certain position must have several properties; the gradient of the signal must be zero in the position and it must not vary too much with position so that samples with slightly different lengths can be measured without having to apply large corrections. Furthermore, different positions must give significantly different values of the parameters of equation 5.

The measurements contain two parts: determination of the influence functions of different materials in order to choose some suitable positions, and determination of s_1 for standard materials in these positions.

5.1. Influence Functions

The influence functions (also called the statistical weight) are measured with samples of 20 mm length. Some characteristic curves are shown in fig. 10. It is seen that there are two positions of interest (in the sense defined above) namely the core centre and, depending upon the material, a position some 100 to 130 mm from this point, corresponding roughly to the maximum of the gradient of the neutron flux, and hereafter called the position of "gradient maximum".

FIG. 12

INFLUENCE FUNCTIONS IN THE THROUGH TUBE

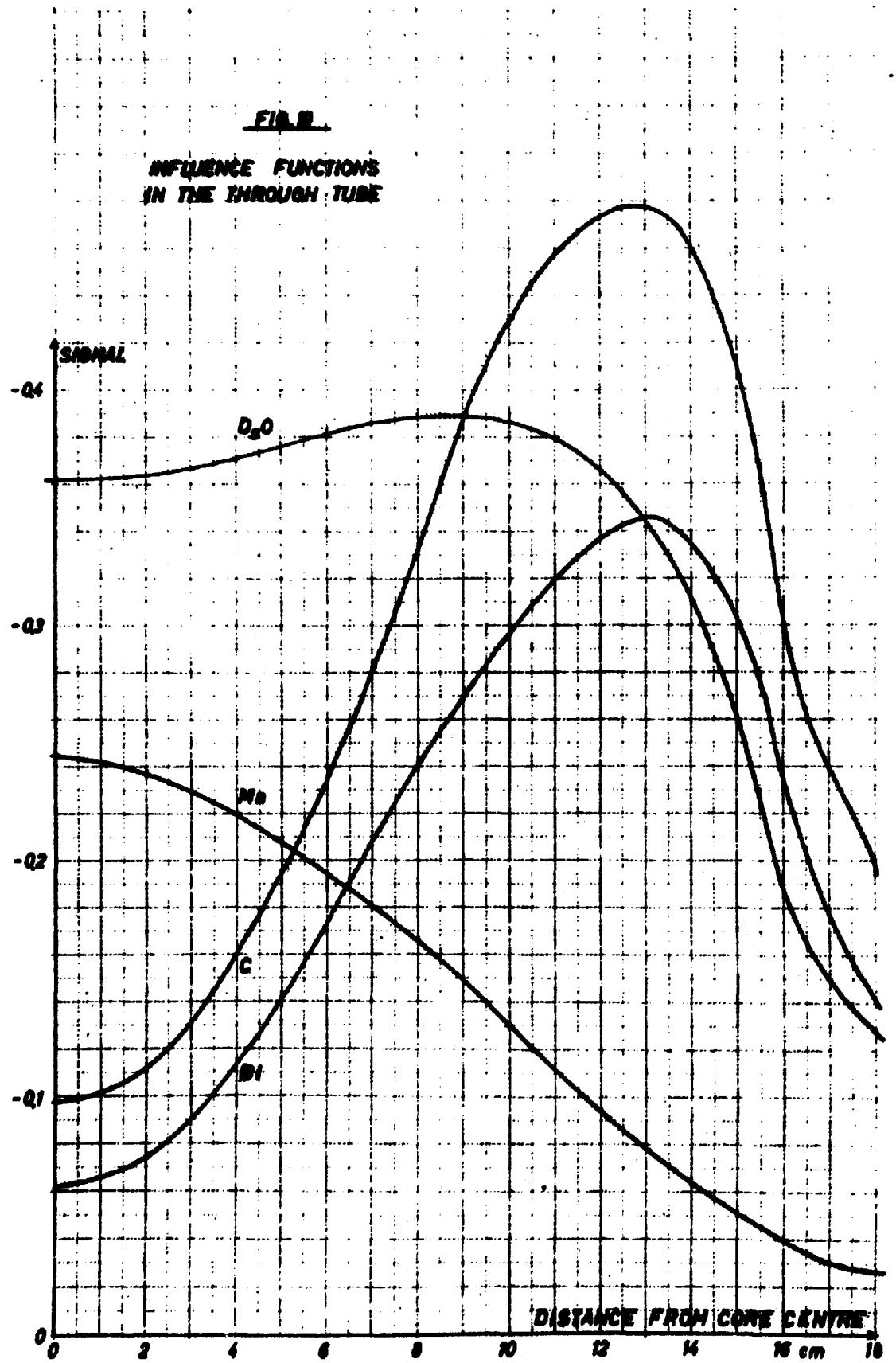

The core centre is the obvious position in which to make the measurement, because the gradient of the flux is zero since the centre is a symmetry point. Here the absorption mainly is responsible for the signal, but because of the rather hard spectrum the slowing down also gives a significant contribution. The scattering has no significant effect because of the symmetry. Thus a superposition of two effects is measured.

At a position about 125 mm from the centre of the core, the signal from a scatterer was found to be maximum. From fig. 10 it is seen that this position depends on the sample, but for obvious reasons just one point was chosen for all measurements. It is also seen that the width of the peak is somewhat narrower than the width in the centre, meaning that shorter samples must be used in order to avoid end corrections.

5.2. Calibration

The calibration at the core centre was performed with samples of 50 mm length and at the gradient maximum with samples of 20 mm length.

These lengths were determined by the influence function. Identical lengths could, of course, have been used, but the use of different lengths does not complicate the procedure as measurements are seldom performed in the gradient maximum.

The samples chosen for the calibration (shown in table I) had well-known properties, were easy to handle and to obtain in a pure form.

Table I

Cross sections for elements used in the calibration
(All values given in barns)

Element	σ_a^{2200}	σ_s	$\xi\sigma_s$	$\sigma^G_{a,\,eff}$	$\sigma^L_{a,\,eff}$
Be	0.01	7.00	1.455	0.01	0.01
B	767	4.0	0.684	767	767
C	0.0037	4.8	0.692	0.0037	0.0037
S	0.52	1.1	0.067	0.57	0.57
Mn	13.2	2.3	0.125	14.43	13.68
Fe	2.62	11	0.388	2.74	2.69
Cu	3.85	7.2	0.222	4.15	4.07
Bi	0.036	9.0	0.086	0.042	0.039
D_2O x)	-	0.408	0.147	0.00003	0.00003
Pb	0.171	7	0.067	0.177	0.174

x) Values refer to Σ/ϱ

$\sigma^G_{a,\,eff}$: $\hat{\sigma}_a$ in the global oscillator assuming r = 0.103

$\sigma^L_{a,\,eff}$: $\hat{\sigma}_a$ in the local oscillator assuming r = 0.053

B, Fe, Cu and Mn are mainly absorbers, C, S, Pb and Bi are scatterers, while D_2O, Be and C are moderators. The boron was measured in form of H_3BO_3 in heavy water.

The cross sections used for the calibration (shown in table I) were found in refs. 2.1 and 2.2. They were corrected for the neutron temperature and for the epithermal neutrons.

The signals, s_1, and variances, were worked out according to section 3 and are given in table II.

In table III the results of the fitting procedure according to equation 5 are given. The results depend somewhat upon the materials used for the calibration, i.e., the set of measurements and/or cross sections is not quite consistent. However, the listed sets were selected to be the standard sets.

Table II

Results of measurements.
Global and local oscillator

Element	a_1(core centre)	a_1(gradient max.)	a_1(local)
Be	-0.2974 ± 0.0125	-0.3885 ± 0.0057	+0.0070 ± 0.0002
B	+ 642.5 ± 13.4	+ 158.1 ± 2.2	- 35.95 ± 0.45
C	-0.0852 ± 0.0078	-0.2246 ± 0.0024	+0.0025 ± 0.0001
S	-0.1436 ± 0.0012	+0.0232 ± 0.0024	-0.0084 ± 0.0001
Mn[x)]	+1.9995 ± 0.0227	+0.6804 ± 0.0238	-0.1113 ± 0.0002
Fe	+0.3523 ± 0.0041	+0.0789 ± 0.0124	-0.0229 ± 0.0004
Cu	+0.4997 ± 0.0458	+0.0833 ± 0.0218	-0.0281 ± 0.0020
Bi	-0.0883 ± 0.0001	-0.0282 ± 0.0010	+0.0002 ± 0.0001
D_2O	-0.4696 ± 0.0185	-0.4160 ± 0.0040	+0.0104 ± 0.0003
Pb	-	-	-0.0003 ± 0.0001

[x)] Measured as Mn-Ni containing 88% Mn.

Table III

Parameters of equation (5)

	α	β	γ
Core centre	+13.56 ± 0.25	-0.134 ± 0.109	-2.154 ± 0.206
Gradient maximum	+3.829 ± 0.257	-0.950 ± 0.095	-0.138 ± 0.349
Local	-0.8155 ± 0.019	+0.0024 ± 0.0015	+0.0562 ± 0.0083

The values of the parameters in table III depend on the oscillator period and upon the apparatus, because they are normalized with a certain percentage of the neutron level. They will also depend somewhat upon the type of sample containers used, both because the sample container changes the neutron spectrum and the neutron streaming in the oscillator channel

varies. A further discussion of this problem is given in section 9.

It is seen from the ratio between α, β and γ that in the centre of the core, the signal depends mainly upon the absorption, but the contribution is not insignificant from the slowing down. This contribution is to be expected since the spectrum is rather hard. The scattering does not contribute significantly because the centre is a symmetry point.

In the gradient maximum (125 mm from the core centre) absorption does not play as great a role as in the centre, while the scattering is quite significant. The slowing down is almost negligible.

Thus it is possible to use two positions having different properties. This means that a considerable amount of information can be extracted from measurements with the global oscillator.

5.3. Some Calculations of the Signals

Some calculations of the calibration formula in the global oscillator have been performed using simple two-group theory. First the fluxes, real and adjoint, were computed on the basis of the geometry and the composition of the reactor. Next these fluxes were put into usual perturbation theory expressions and, when the resulting reactivities were multiplied by the amplification of the system, the formula below were found:

$$S_c = 17.20 \frac{\Sigma_a}{\xi} - 1.28 \frac{\xi \Sigma_s}{\xi} \qquad \text{(centre)}$$

$$S_g = 6.98 \frac{\Sigma_a}{\xi} - 0.484 \frac{\xi \Sigma_s}{\xi} - 0.352 \frac{\Sigma_{tr}}{\xi} \qquad \text{(gradient max.)}$$

the coefficients of which are to be compared with the constants in table III.

It is seen that the discrepancies are considerable. It is believed that they are caused by the difference between the actual system and the model used for calculation; in particular, the through-tube has not been taken into account.

6. The Local Oscillator

The local oscillator is based on an annular ionization chamber placed in the reflector. The sample moves in and out of the chamber which in turn detects the flux perturbation.

Of course, there is some coupling between the sample in the local oscillator and the reactor, i. e. there is some additional global flux perturba-

tion, but it is normally insignificant.

6.1. Ionization Chamber

The annular, boron-lined ionization chamber in current use was designed at DR 1. Filled with argon at atmospheric pressure, it has been working satisfactorily for more than a year. However, the integrated dose is rather low and the behaviour at higher doses cannot therefore be predicted.

Fig. 11 gives a drawing of the chamber and a photograph of it is seen in fig. 1C. The outer diameter is determined by the dimension of the reflector channel into which the chamber must fit. The inner diameter is a compromise between the desire to have fairly large samples and the need to have room for the electrodes. The length of the chamber is determined by the length of the sample so that the signal from the sample can be independent of the position within reasonable limits. Thus an electrode length of 200 mm was chosen as suitable for a 50 mm sample length.

Calculations have shown that the thickness of the boron layer is not critical and the optimum is around 1 mg/cm^2. This thickness has been used by several authors [4.1, 4.2, 11].

Calculations have shown[8] that the thickness is a compromise between the fraction of the α-particle energy which contributes to the ionization and the fraction of neutrons absorbed in the boron. A thin boron coating will permit a large fraction of the α-particle energy to ionize the gas, but only few neutrons will be absorbed. A thick coating will absorb many neutrons, but only few of the α-particles will ionize the gas and, in addition, the coating will shield the sample which thus has little effect on the neutron flux. A marked improvement of the α-particle efficiency is gained if enriched boron is used.

Some authors prefer to have several layers of boron as this increases the sensitivity of the chamber, but this complicates its structure.

The chamber consists of one signal electrode with a mean thickness of 1.5 mg/cm^2 boron on each side, and two high tension electrodes.

The boron was applied in the following manner: The aluminium electrode to be coated was etched with a mixture of phosphoric acid and nitrogen acid (1 : 5). The solution was left for an hour (not critical) after which the electrode was rinsed and dried. The surface was then full of pitches. The boron (electrolytically purified, but amorphous may be used as well) was ground very thoroughly in a mortar wetted with white spirit, in order to obtain fine grains. When changes in the grain size could not

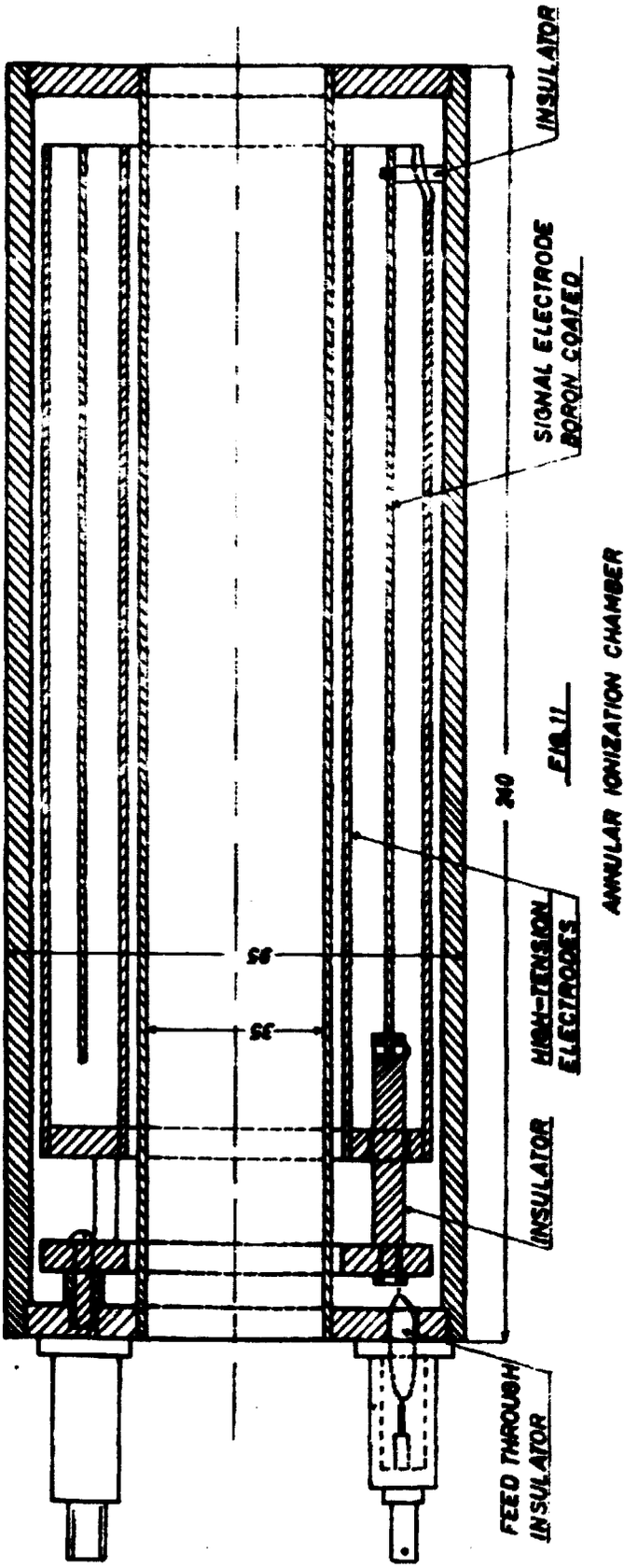

ANNULAR IONIZATION CHAMBER

longer be "felt", the boron was ready for application.

An electrode was fixed in a slowly turning lathe and the boron, suspended in white spirit, was brushed onto the surface until it appeared uniformly grey-black. A heating lamp was used for swift evaporation of the white spirit, whereafter the electrode was weighed and the boron thickness calculated. If necessary the layer was thickened.

After the final application of boron, the cylinder was heated for an hour at a temperature of about 300°C in order to fix the layer, but it is doubtful whether this treatment had any effect. At all events, the electrode could be smacked onto a table without any boron being dislodged, but of course, the layer could be easily wiped off. Evaporation of solid boron or decomposition of boron gas onto the electrode surface could improve the method, but both these processes are more complicated than the simple painting.

The electrodes are fixed in the chamber with teflon insulators. The insulation resistance between the electrodes was 10^{13} ohms before the chamber was irradiated.

The feed-through insulators are of glass, and the flash-over voltage is some 1 kV.

Because of the nature of the materials used, the chamber could not be welded and therefore it was finally assembled with cement. After evacuation for several hours it was filled with argon and sealed off by flattening of the gas tube.

The chamber was examined by measuring the current versus the neutron density, and the current versus the polarizing voltage. There was linearity between current and flux at least up to 50 μA, and the current was independent of the high tension between 50 and 500 volts (see fig. 12). The neutron sensitivity was around 10^{-14} A/(n/cm^2/sec). The γ-sensitivity was measured on a similar chamber using a cobalt-60 source, and was found to be 4×10^{-11} A/R/h. The influence of the γ-sensitivity is seen on fig. 12.

Presumably this chamber cannot be used in high fluxes where the glass insulators could break down. Furthermore, the cement and teflon will be destroyed by a high integrated dose. A new type is in preparation in which ceramic insulation is used. Furthermore, the boron is applied by decomposing a boron gas (B_2H_6), whereby the layer is quite uniform.

6.2. Influence Functions

The first properties of the oscillator to be measured were the signal

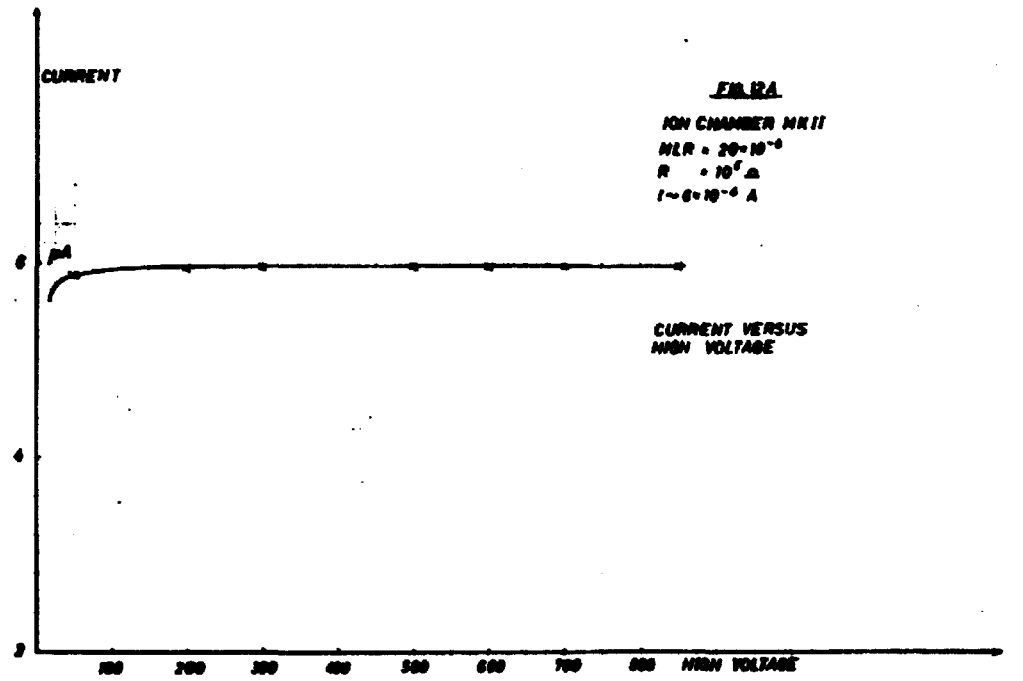
CURRENT
FIG 12A
ION CHAMBER MK II
NLR = 20×10⁻⁶
R = 10⁶ Ω
I ~ 6×10⁻⁶ A
μA
6
4
2
CURRENT VERSUS
HIGH VOLTAGE
HIGH VOLTAGE

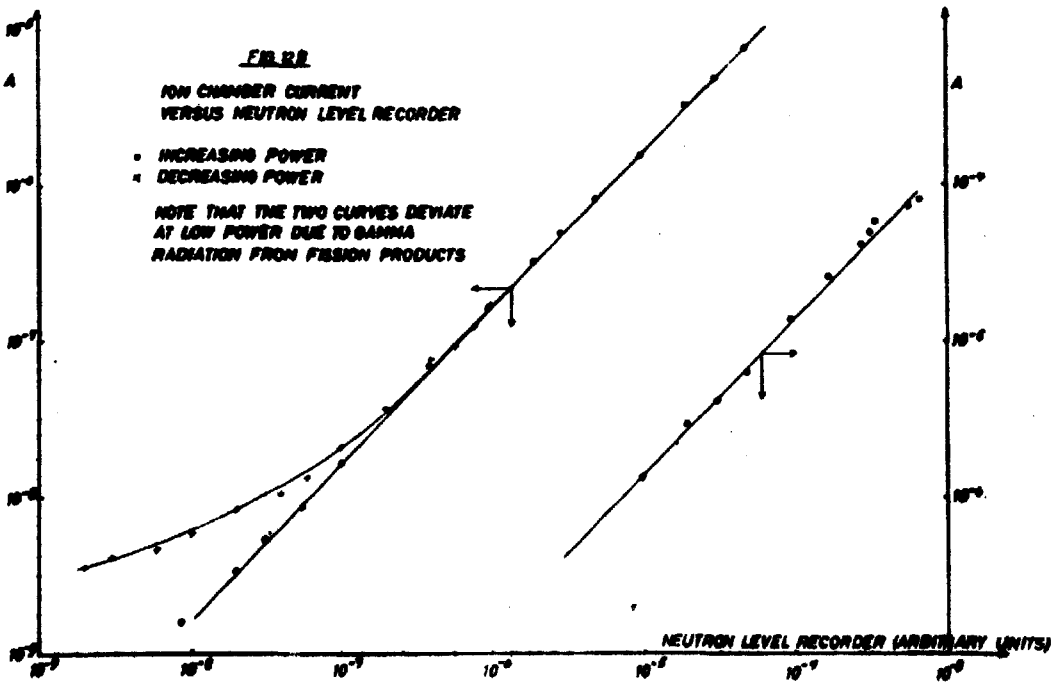
FIG 12B
ION CHAMBER CURRENT
VERSUS NEUTRON LEVEL RECORDER
• INCREASING POWER
× DECREASING POWER
NOTE THAT THE TWO CURVES DEVIATE
AT LOW POWER DUE TO GAMMA
RADIATION FROM FISSION PRODUCTS
A
NEUTRON LEVEL RECORDER (ARBITRARY UNITS)

versus the position of different types of probes: an absorber, a scatterer, and a moderator. The curves in fig. 13 give some of the most important results. It is seen that the signal from an absorber is almost constant through the chamber, while the signal from a scatterer is rather varied.

It is seen that a suitable length for the sample is 5 cm, as was planned when the chamber was designed. The curves are not quite symmetric due to the asymmetric set-up. In particular, the scattering gives rise to asymmetry. This is not very significant if the sample is short, but to examine the space dependance more closely, calibrations were made in positions 110, 120, and 130 mm from the bottom of the chamber.

It may be possible to flatten the influence functions somewhat, especially for the scatterers, by extending the boron layer to both sides of the chamber in order to make the set-up more symmetric.

6.3. Calibration

The local oscillator was calibrated in the same way as the global oscillator. When possible the samples were 5 cm long. However, some measurements were also performed in order to check the influence of the length of the sample.

The materials considered are given in table I and are the same as those used in the global oscillator. The effective cross sections are not the same as those in the centre of the core, both because of a softer spectrum in the reflector and because of a somewhat lower neutron temperature. A temperature of 40°C was used measured by use of the sandwich technique with gold foils, but accuracy was rather poor. New measurements using the oscillator itself are in progress.

Samples with different masses were measured, and the results processed as mentioned above. These are given in table II.

The boron samples were measured both as a solid, applied in a thin layer on aluminium tubes, and as a liquid, dissolved in D_2O in the form of H_3BO_4. Three concentrations were used: 0.928, 0.484, and 0.230 mg B per gram solution. In addition, a sample of the D_2O used was measured in order to obtain corrections for the increased flux due to slowing down. The sample containers were filled in a dry-box, but the successive change of the sample size was performed without any special precautions other than swift handling. The results showed no significant contamination with H_2O. The flux peaking due to the slowing down of fast neutrons in the D_2O was found to be some 2%.

FIG.13

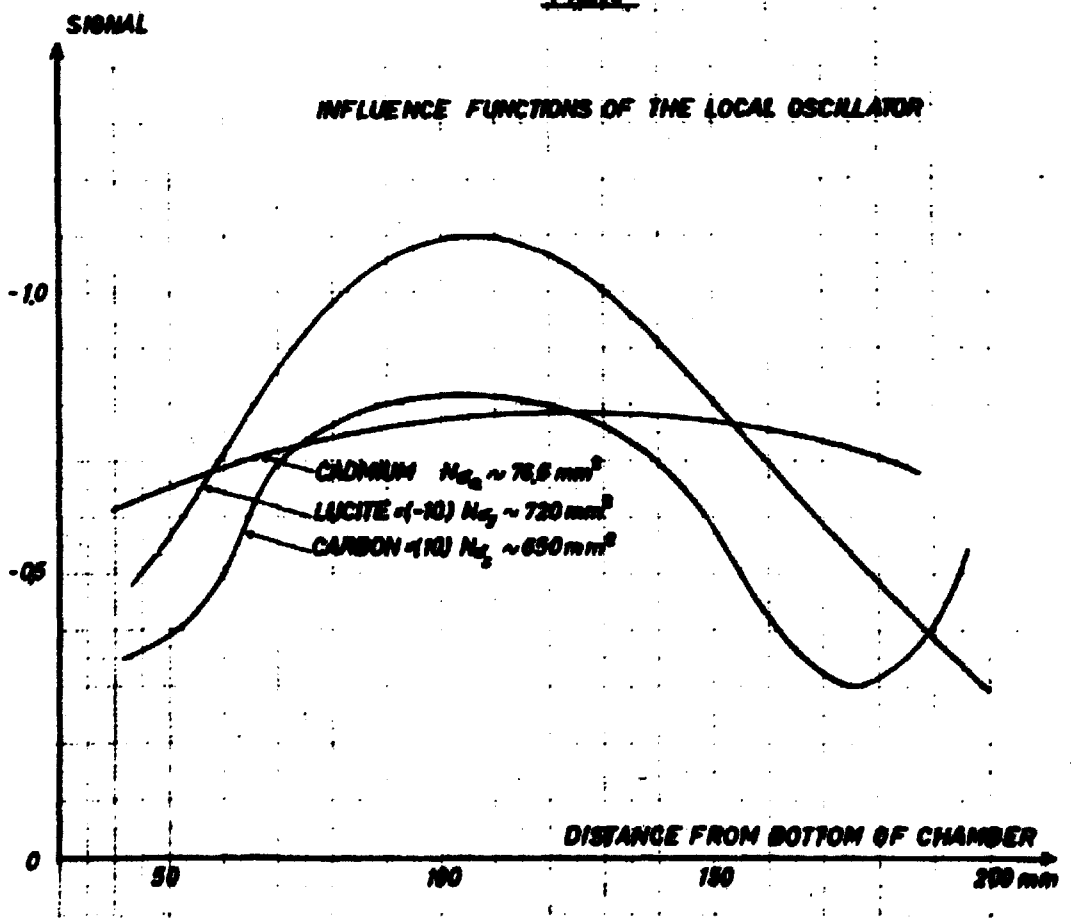
SIGNAL
INFLUENCE FUNCTIONS OF THE LOCAL OSCILLATOR
-1.0
-0.5
0
CADMIUM
LUCITE
CARBON
50
100
150
200 mm
DISTANCE FROM BOTTOM OF CHAMBER

The results of the measurements were fitted to formula (5) and the parameters considered to be the best are given in table III. It was found that the variation with position is rather slow, which means that the samples need not be placed very accurately. A half millimeter tolerance seems to be acceptable.

7. Standards

It is still an open question whether to use a standard or not, since much depends upon the actual circumstances.

A standard is a certain sample which is measured each time a material is examined and, if possible, in the same container. The standard may consist of any material, the only necessities being that it is easy to handle and has a stable surface.

All measurements may be divided by the signal from the standard. In this way any long-time change in the whole set-up, including the reactor, is assumed to be cancelled.

Of course, if the oscillator is quite stable there is no need to use a standard. Furthermore, any short-time change in the set-up gives a variation of output and therefore the standard cannot be relied upon either. Thus it may be concluded that the standard is of most use as a check on the stability of the equipment.

However, if measurements from different oscillators are to be compared, a standard is necessary, e. g. because of difference in transfer functions and neutron spectra. In addition, if the oscillator's analyzing equipment is changed, the standard is important.

Because of its nuclear properties (no resonance, 1/v-absorption) boron is preferable as a primary standard, i. e. all measurements are referred to a certain amount of boron. On the other hand, boron is difficult to handle, e. g. it has to be measured dissolved in D_2O. Therefore a secondary standard, say an aluminium cylinder, is often calibrated in terms of the boron signal.

It may be of interest to have a standard for scattering and moderating properties also. D_2O seems obvious, but it is difficult to handle because of the possibilities of contamination with H_2O. Again aluminium may be used as a secondary standard.

If there is neutron streaming in the channel where the measurements are performed, the signal of a sample (including the standard) may depend

upon the sample container. However, the ratio between the sample and the standard will not be influenced by the container.

Some typical measurements of a standard are given in table IV.

Table IV

Standard Al A63

Dimensions	48.5 x 10$^{\emptyset}$ mm, 17.432 g, Al 2S
Signal core centre	+ 0.8130 $\pm$ 0.0015 (average of 9 measurements)
Signal gradient maximum	- 0.5073 $\pm$ 0.0016 (" " 9 ")
Signal local oscillator	- 0.0782 $\pm$ 0.0014 (" " 14 ")

8. Comparison of the Oscillators and Proposed Improvements

Besides the principal differences in the way the two oscillators work, they give possibilities of separating a total absorption cross section in two parts, namely a thermal and a resonance part. If the scattering cross section is not known, one may get a rough indication of it from the effective cross section measured in the gradient maximum.

The sensitivities of the two systems are nearly the same.

In the global oscillator some rather annoying streaming is present, making the scattering cross section of materials like aluminium and magnesium appear to be large, thus complicating the determination of the absorption cross section. This is not the case in the local oscillator.

The slowing down plays a significant role in the global oscillator. However, the hard spectrum makes it possible to measure resonance integrals.

The thermal cross section measurements could be improved if the local oscillator was placed in a still softer spectrum, e. g. a thermal column. Also a neutron source (a reactor) with lesser noise would be useful. It appears that the noise in the oscillator stems mainly from the reactor; this was observed when a neutron source was oscillated at approximately zero reactor power (< 0.1 W) in which case there was hardly any noise. A reactor with solid fuel is considered to be quieter than a homogeneous reactor,

due to the avoidance of bubble formation.

There are two improvements which have been carried out or proposed by other authors.

One concerns the local oscillator only. The signal is proportional to the mean neutron level, and if it varies the signal will be affected. If another ionization chamber is placed in such a position that it is insensitive to the local effect it may provide reference (back bias), and thus any variation of the neutron level around the average will be compensated [12].

The second improvement embodies simultaneous running of the two oscillators in the following way. The annular ionization chamber is placed in a zone where the global influence function is significant. Another chamber which detects the global effect only is connected to a fast automatic power control. In this case, the mean level of the reactor will be constant irrespective of the position of the sample, due to the global regulator, while the local oscillator will work in the normal way. The output of the power regulating system serves as the global oscillator output[13].

9. Flux Measurements

In order to determine the effective absorption cross section of the samples, the Westcott formalism was used:

$$\hat{\sigma} = \sigma_o (g + rs) \tag{6}$$

Both the epithermal index r and the neutron temperature T_n must be known, because g and s depend on T_n.

The epithermal index r is determined through the following formula given in ref. 3

$$r \sqrt{\frac{4T_n}{\pi T_o}} = \frac{g}{\frac{\sigma_{res} - m}{\sigma_o} \; CR - S\sqrt{\frac{\pi T_o}{4T_n}}} \tag{7}$$

where CR is the cadmium ratio for infinitely thin detectors, and m is determined by the cut-off function :

$$m = \int_{0.55\ ev}^{E_{cd}} \sigma(E) \frac{\Delta}{E} \, dE \tag{8}$$

Some rough measurements have been performed that indicate a neutron temperature of approximately 60°C in the core, and the temperature at the local oscillator is estimated to be approximately 40°C.

All the flux measurements have been performed with gold foils with or without a cadmium cover (about 1 mm thick). The measurements of the activities have been carried out by means of a scintillation counter and of a 4π-β-γ-coincidence counter.

The fluxes and the r-values are given on fig. 14. It is seen that the spectrum is hard, $r \sim 0.1$, in the core, while it is softer, $r \sim 0.05$, at the local oscillator.

These data have been used in connection with cross sections from ref. 21 and 22 to obtain the effective cross section given in table I.

10. Additional Measurements

Some measurements of neutron sources have been performed in order to determine the significance of neutrons of different energies, which is of importance when fissile materials are examined.

When fissile materials are measured in the oscillators, the neutrons from the induced fissions give rise to a certain signal. The signal may be written:

$$S = \alpha\Sigma_a/\varrho + \beta\Sigma_s/\varrho + \gamma\,\xi\,\Sigma_s/\varrho + \varkappa(E)\;\Sigma_f/\varrho \qquad (5A)$$

where

$\varkappa(E)$ is a weight factor depending on the spectrum of the neutrons from the sample,

Σ_f/ϱ is the fission cross section of 1 gram of the sample,

and the other quantities are identical to those given in formula (5).

In order to determine $\varkappa(E)$ the signal from different types of neutron sources has been measured. It may be shown that

$$S(\text{source}) = A + \varkappa(E)\,\frac{Q(E)}{\Phi} \qquad (5B)$$

where

A is a constant depending on the absorption and scattering of the neutron source,

Q (E) is the source strength of a source with neutron energy E

and

Φ is the neutron flux (nv_o) at the position of the source.

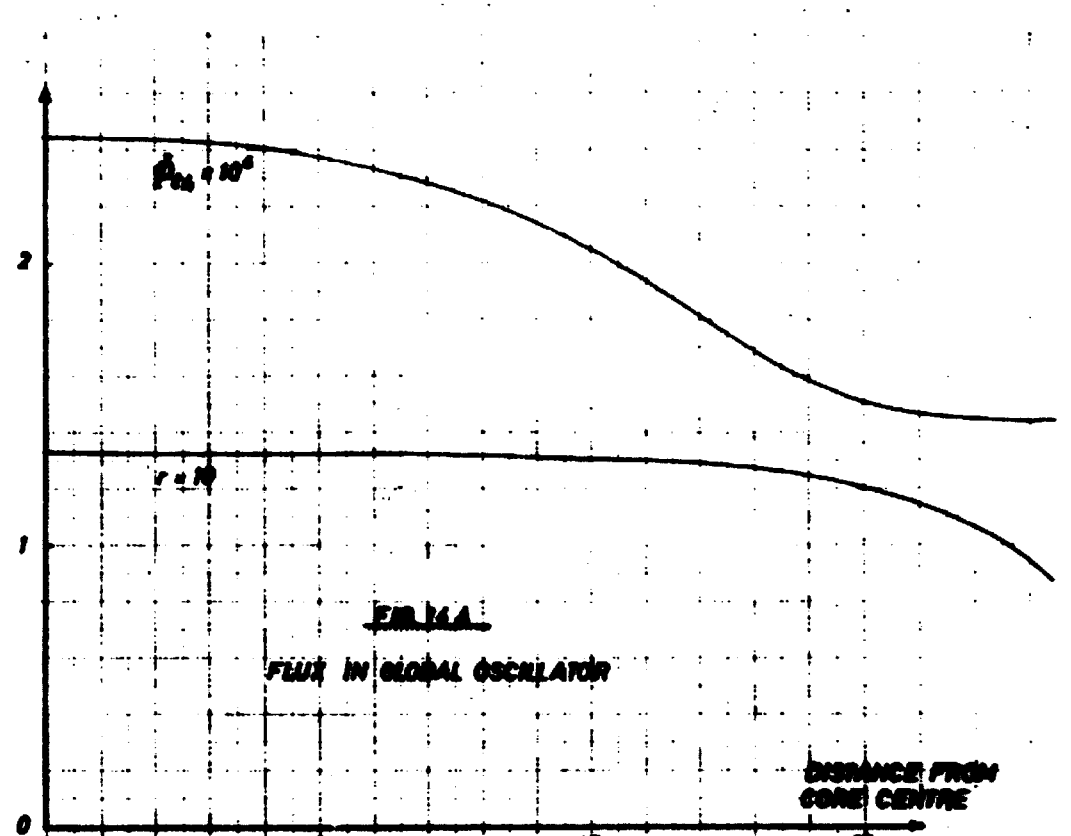

FIG 14 A

FLUX IN GLOBAL OSCILLATOR

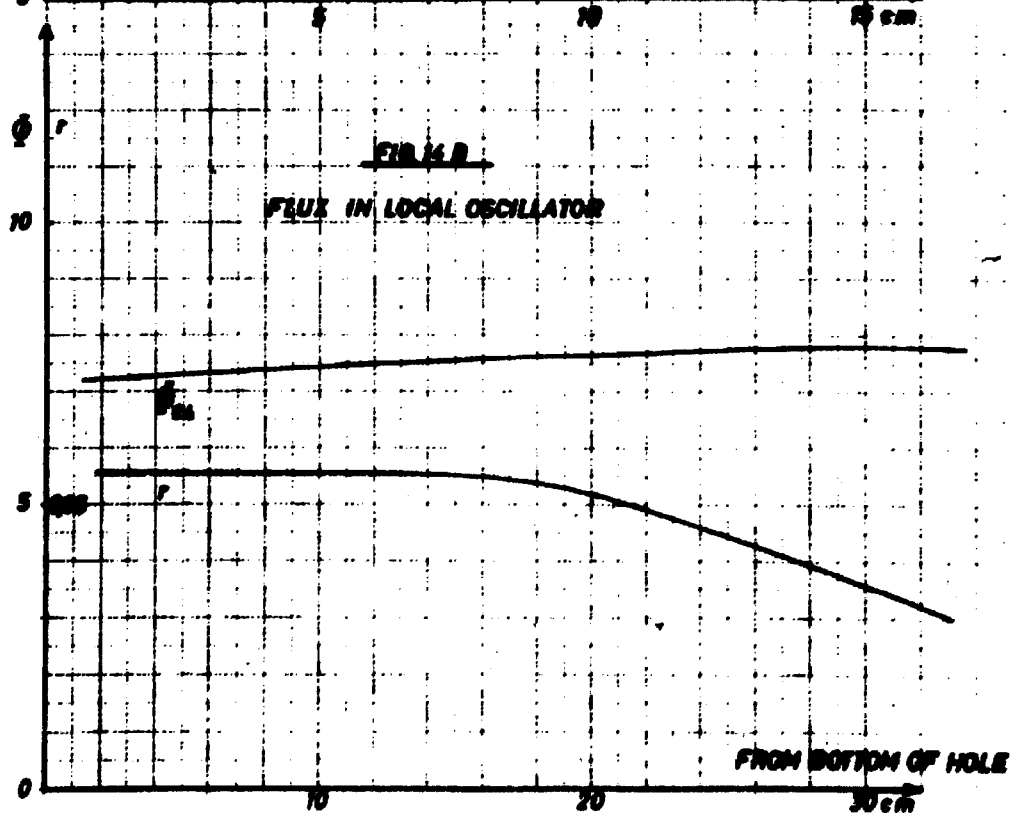

FIG 14 B

FLUX IN LOCAL OSCILLATOR

Equation (5B) allows the determination of the connection between the signal and the source strength. Having sources of different energies, $\varkappa(E)$ may be estimated. The following values have been found:

$\varkappa(E)$ for different neutron sources

Source	Ra-Be	Sb-Be
Core centre	7.6 ± 0.5	6.2 ± 0.5
Local oscillator	7.0 ± 0.5	-

Acknowledgements

The author expresses his sincere thanks to P. L. Ølgaard for his critical review of this manuscript. He also expresses his thanks to J. Olsen for stimulating discussions and he is most indebted to the staff of DR 1, who patiently performed the experiments and calculations, and gave him much valuable advice.

References

1. Construction and Operation of Research Reactor DR 1. P. Frederiksen. Risö Report No. 10 (1959).

2.1. Effective Cross Section Values for Well-Moderated Thermal Reactor Spectra. C. Westcott. AECL 1101 (1962).

2.2. Pile Oscillator Measurements of Resonance Absorption Integrals. R. Tattersall et al. AERE-R 2887 (1959).

3. Measurements of the Thermal and the Epithermal Neutron Flux in the Reactor DR 1. B. Fastrup and J. Olsen. Risö Report No. 43 (1962).

4.1. Measurements of Thermal Neutron Absorption Cross Sections with a Pile Oscillator. T. Fuketa and S. Otomo. JAERI 1009 (1960).

4.2. A Modified Oscillator for Neutron Cross Section Measurements. J. Anno, R. Jung and J. Chastain. BMI 1265 (1958).

5. Measurements of the Change in Cross Section of Irradiated Uranium made by Modulating the Power of a Nuclear Reactor. D.J. Littler. AERE RS/R - 2092 (1956).

6. En kinetisk model af DR 1 (A Kinetic Model of DR 1). P. Kirkegaard. Master Thesis (1961).

7. The Transfer Function of a Water Boiler. R. Skinner and L. Hetrick. NAA-SR-1948 (1957).

8. Fremstilling af annulært, borforet ioniseringskammer. (On the Manufacture of an Annular Boron-coated Ionization Chamber). O. Rasmussen. Master Thesis (1965).

9. Ein Globaler Pileoszillator am Rossendorfer Forschungsreaktor. P. Liewers. Kernenergie, vol. 6, 263 (1963).

10. The Calculus of Observations, 3rd Edition. E.T. Whittaker and G. Robinson. (Blackie, London, 1940.)

11. Ein Lokaler Pileoszillator zur Thermischer Absorptions Querschnitte am RFR. G. Hüttel und P. Liewers. Kernenergie, vol. 6, 336 (1963).

12. A Paired Chamber Type Pile Oscillator. T. Fuketa. Nuc. Instr. and Meth., vol. 13, 35 (1961).

13. **Mesure des sections efficaces effectives d'echantillons fissiles par une methode d'oscillation dans les assemblages critiques. R. Vidal, O. Trediakoff et M. Robin. Exponential and Critical Experiments, Vienna, IAEA, 1964, vol. 3, pp. 141-161.**